

# Solubility of 2,5-Furandicarboxylic Acid in Pure and Mixed Organic Solvent Systems at 293 K Predicted Using Hansen Solubility Parameters

Jacob M. Molinaro, Matthew R. Carroll, Annabelle S. Young, and Stephanie G. Wettstein\*



Cite This: *ACS Omega* 2024, 9, 30708–30716



Read Online

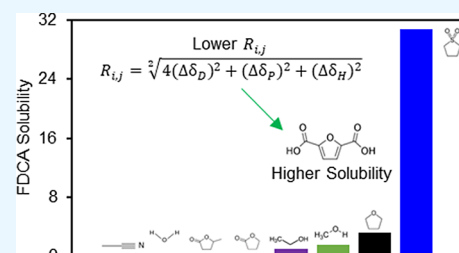
ACCESS |

Metrics & More

Article Recommendations

Supporting Information

**ABSTRACT:** Central to the production of polyethylene furanoate (PEF), a bioplastic that could potentially replace petroleum-derived plastics, is 2,5-furandicarboxylic acid (FDCA). FDCA is a chemical derived from biomass that has low solubility in traditionally used solvents such as water. Thus, identifying solvents that can solubilize significant amounts of FDCA could allow for lower PEF production costs. In this study, FDCA solubility was investigated in nine pure solvents including H<sub>2</sub>O, acetonitrile (ACN),  $\gamma$ -valerolactone (GVL),  $\gamma$ -butyrolactone (GBL), ethanol (EtOH), methanol (MeOH), dimethyl sulfoxide (DMSO), sulfolane (SULF), and tetrahydrofuran (THF), eight binary, and three ternary solvent blends at 293 K. For all binary systems excluding DMSO and MeOH, the solubility of FDCA increased 1.5–65 times compared to the pure organic solvent, and the FDCA solubility was at least 10 times higher when compared to pure water. Specifically, the 20/80 w/w H<sub>2</sub>O/DMSO system solubilized 23.1 wt % FDCA, the highest of any binary blend studied, and 190 times more solubility than in pure water. In 20/80 w/w H<sub>2</sub>O/THF, the FDCA solubility was 60 times higher than pure water. In ternary blends that included DMSO, H<sub>2</sub>O, and either GVL, THF, or SULF, solubility increased by at least 6.6 times relative to the pure secondary organic component and 54 times relative to pure water. Using Hansen solubility parameters (HSPs), the radius of interaction ( $R_{i,j}$ ) was found to be more strongly correlated to FDCA solubility than individual HSPs or the total solubility parameter. A MATLAB-based optimization code was developed and successful in minimizing the  $R_{i,j}$  of a solvent blend to maximize FDCA solubility in binary and ternary aqueous solvents.



## INTRODUCTION

As a biomass-derived platform chemical, 2,5-furandicarboxylic acid (FDCA) has diverse applications that could help build a sustainable future. With the diminishing availability of nonrenewable resources, there is a growing emphasis on sustainable production methods for consumer goods. One area affected by this is the petrochemical and plastics industry, as everyday products like food containers, shipping packaging, and water bottles are made from polyethylene terephthalate (PET).<sup>1</sup> Although extremely useful, PET products are manufactured from petroleum derivatives and are significant contributors to pollution and long-term environmental damage when not recycled.<sup>2</sup> One solution to this problem is the introduction of biobased plastics like polyethylene furanoate (PEF),<sup>3</sup> which can be synthesized from lignocellulosic biomass-derived FDCA. The economical production of FDCA is of great importance to PEF production, but the low solubility of FDCA<sup>4–7</sup> presents a challenge. In solvents such as water<sup>4</sup> and ethanol,<sup>8</sup> the solubility of FDCA is less than 1 wt % at STP. Therefore, either large amounts of solvent or additives, like sodium hydroxide, are required to improve solubility, which increases the financial barrier to scale up.<sup>9,10</sup>

Although the literature is limited, research has reported that organic solvents show promise for improving FDCA solubility.

Zhang et al.<sup>5</sup> reported FDCA solubilities in eight pure and two binary mixtures from 313 to 363 K and correlated increased solubility to increased temperature. Additionally, mixtures achieved higher solubilization of FDCA than pure components. For example, at 323 K the FDCA solubility in acetic acid (AA) and acetonitrile (ACN) were 0.09 and 0.04 wt %, respectively, which is lower than the solubility they reported in pure water (0.25 wt %). However, in aqueous/organic mixtures, the maximum reported solubilities were 0.70 wt % (at 40/60 w/w H<sub>2</sub>O/AA) and 2.5 wt % (at 39/61 w/w H<sub>2</sub>O/ACN), representing at least a two-fold increase over pure components. Thermodynamic models were able to predict the H<sub>2</sub>O/AA and H<sub>2</sub>O/ACN binary mixture solubility data using both the nonrandom two-liquid (NRTL) and universal quasichemical (UNIQUAC) models.<sup>5</sup>

In other studies by Motagamwala et al.<sup>4</sup> and Ban et al.,<sup>8</sup> similar or higher FDCA solubilities were observed. In a 20/80

Received: April 2, 2024

Revised: May 2, 2024

Accepted: June 27, 2024

Published: July 5, 2024



w/w H<sub>2</sub>O/ $\gamma$ -valerolactone (GVL) solvent system, Motagamwala et al. increased FDCA solubility an order of magnitude from 0.2 wt % in pure water to 2.4 wt % at 303 K. At 373 K, the same solvent blend solubilized over 9 wt % FDCA compared to just over 1 wt % in pure water. They hypothesized that the increase in solubility within binary aqueous/organic mixtures was related to a higher enthalpy of mixing between solvents.<sup>4</sup> Ban et al. studied binary mixtures of H<sub>2</sub>O/AA, H<sub>2</sub>O/ethanol (EtOH), and H<sub>2</sub>O/methanol (MeOH). Findings showed that for AA, binary mixtures yielded higher solubility than the pure component, but that MeOH and EtOH both showed the highest solubility as pure components, although the range of mixtures studied only included 0–30 wt % H<sub>2</sub>O.<sup>8</sup>

Zhuang et al.,<sup>6</sup> in a similar study, found that all binary aqueous/organic mixtures they studied (tetrahydrofuran (THF), 1,4-dioxane (DX), 1,2-dimethoxyethane (DME), and diethylene glycol dimethyl ether (DGDE)) had higher solubility than pure components. They proposed the use of several thermodynamic models, including Hansen solubility parameters (HSPs), to provide a useful approach for finding ideal solvents. Specifically, using the Hansen Total Solubility Parameter,  $\delta_T$ , a strong correlation was found between solvents and solutes of similar  $\delta_T$  and FDCA solubility.

Compared to NRTL and UNIQUAC models, HSPs are convenient since data for thousands of common solutes and solvents are available, mixtures of solvents can be easily considered, and they can be adjusted for temperature. HSPs were originally developed to assess solvent compatibility within the paint and coatings industry, where they were found to be effective for developing surface coatings.<sup>11</sup> Since then, HSPs have been effectively applied for selecting green extraction solvents,<sup>12</sup> cellulose solubilization solvents,<sup>13</sup> and ideal solvents for lignin dissolution.<sup>14</sup> Despite this, to the best of the authors' knowledge, no further work has been done applying HSPs to FDCA solubility beyond that reported by Zhuang et al.<sup>6</sup> It is hypothesized that by identifying what HSP parameter correlates best to FDCA solubility solvent blends could be optimized, leading to improved efficiency in PEF production. Additionally, the findings presented herein may apply to solute–solvent combinations at a much broader scale.

For this work, nine solvents were selected based on prior application in the production of furan compounds<sup>15</sup> or the upgrading of HMF<sup>8,16</sup> to determine FDCA solubility in pure and blended solvent mixtures. These solvents were H<sub>2</sub>O, ACN, GVL,  $\gamma$ -butyrolactone (GBL), EtOH, MeOH, dimethyl sulfoxide (DMSO), sulfolane (SULF), and THF. Using these solvents, we not only build upon existing research but also provide new insights into the relationship between HSPs and FDCA solubility and report HSPs and FDCA solubilities for ternary solvent blends.

## THEORY

The work conducted by Motagamwala et al.,<sup>4</sup> Zhang et al.,<sup>5</sup> and Zhuang et al.<sup>6</sup> all cite thermodynamic explanations and correlations for FDCA solubility, specifically correlating solubility to temperature and enthalpy. Such thermodynamic principles state that mixing occurs when there is a negative Gibb's Free Energy ( $\Delta G$ ), which is given for an isothermal system by

$$\Delta G = \Delta H - T\Delta S \quad (1)$$

where  $H$  is enthalpy,  $T$  is temperature, and  $S$  is entropy. Smaller  $\Delta H$  and/or higher  $T$  would thus increase the likelihood of  $\Delta G$  being negative. The enthalpy change ( $\Delta H$ ) can be expressed through HSPs, which decompose  $\Delta H$  into three distinct components: atomic dispersion forces ( $\delta_D$ ), dipole–dipole polarization ( $\delta_P$ ), and molecular hydrogen bonding ( $\delta_H$ ).<sup>17</sup> Each chemical has unique values for these components, which can be found in the literature or are calculable using the HSPiP software.

The HSP dispersion component,  $\delta_D$ , is rooted in nonpolar atomic interactions, also referred to as London dispersion forces. These forces capture fluctuations in the electric field of molecules resulting from interactions with neighboring molecules. The dipole–dipole polarization value,  $\delta_P$ , addresses varying charge densities influencing molecular organization while the molecular hydrogen bonding value,  $\delta_H$ , represents the electrostatic forces between a hydrogen atom and the dipole of another molecule. Both the polarity and hydrogen bonding parameters share a strictly molecular nature, while the dispersion parameter relies on induced dipole interactions with other molecules.<sup>17</sup> HSPs have been previously explored as a promising method for predicting the solubility of many components including FDCA,<sup>6</sup> cellulose,<sup>13</sup> and other ring-containing organic compounds and pharmaceuticals<sup>18–20</sup> with an overall focus on “like dissolves like.”<sup>6,17,21</sup>

The pure component HSP values can then be used to determine the HSPs for solvent mixtures using

$$\delta_{x_{\text{blend}}} = \sum_i (\varphi_i^* \delta_{x_i}) \quad (2)$$

where  $\varphi_i$  is the volume fraction and  $\delta_{x_i}$  is the pure component HSP value. This calculates the mixture values as volume-weighted averages of each component and sets the foundation for further applications in solubility estimation. Then, utilizing the solvent parameters, various methods can be used to estimate solute solubility. One of these methods, which was used by Zhuang et al.,<sup>6</sup> compares the total solubility parameter<sup>21</sup> ( $\delta_T$ ) calculated with

$$\delta_T = \sqrt{\delta_D^2 + \delta_P^2 + \delta_H^2} \quad (3)$$

for both solvent and solute and then calculating the difference between solute and solvent  $\delta_T$  using

$$\Delta\delta_T = \delta_{T,i} - \delta_{T,j} \quad (4)$$

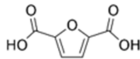

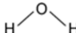
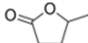
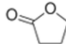
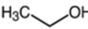
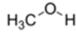

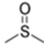
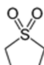
where  $i$  and  $j$  represent the solvent and solute, respectively. According to HSP theory, substances with similar total solubility parameters, and therefore lower  $\Delta\delta_T$  values, are more likely to solubilize each other.<sup>21</sup>

A second method to determine the likelihood of solubilization between a solvent and solute is the radius of interaction ( $R_{i,j}$ ), which is defined as follows:

$$R_{i,j} = \sqrt{4 * (\delta_{D,i} - \delta_{D,j})^2 + (\delta_{P,i} - \delta_{P,j})^2 + (\delta_{H,i} - \delta_{H,j})^2} \quad (5)$$

where  $i$  and  $j$  represent the properties of the solvent and solute, respectively.<sup>21</sup> Similar to  $\Delta\delta_T$ , the lower the value of  $R_{i,j}$  the more likely that the solute is soluble in the solvent.<sup>22</sup> However, the key difference between the two variables is that the  $\Delta\delta_T$  parameter represents an unweighted comparison of each solubility vector, while  $R_{i,j}$  incorporates a weighting factor of 2 on  $\delta_D$ , a coefficient determined through experimental

Table 1. Solvents and Solute Used in Experiments

| chemical name              | chemical abbreviation | CAS No.   | molecular formula                              | structure  | source <sup>a</sup> | purity |
|----------------------------|-----------------------|-----------|--|--|---------------------|--------|
| 2,5-Furandicarboxylic acid | FDCA                  | 3238-40-2 | C <sub>6</sub> H <sub>4</sub> O <sub>5</sub>   |  | AK                  | 98%    |
| Acetonitrile               | ACN                   | 75-05-08  | CH <sub>3</sub> CN                             |  | FS                  | ≥ 99%  |
| Water                      | H <sub>2</sub> O      | 7732-18-5 | H <sub>2</sub> O                               |  | -                   | 18.2Ω  |
| γ-valerolactone            | GVL                   | 108-29-2  | C <sub>5</sub> H <sub>8</sub> O <sub>2</sub>   |  | SA                  | ≥ 99%  |
| γ-butyrolactone            | GBL                   | 96-48-0   | C <sub>4</sub> H <sub>6</sub> O <sub>2</sub>   |  | SA                  | ≥ 99%  |
| Ethanol                    | EtOH                  | 64-17-5   | CH <sub>3</sub> CH <sub>2</sub> OH             |  | AO                  | ≥ 99%  |
| Methanol                   | MeOH                  | 67-56-1   | CH <sub>3</sub> OH                             |  | FS                  | ≥ 99%  |
| Tetrahydrofuran            | THF                   | 109-99-9  | C <sub>4</sub> H <sub>8</sub> O                |   | FS                  | ≥ 99%  |
| Dimethyl sulfoxide         | DMSO                  | 67-68-5   | C <sub>2</sub> H <sub>6</sub> SO               |   | SA                  | ≥ 99%  |
| Sulfolane                  | SULF                  | 126-33-0  | C <sub>4</sub> H <sub>8</sub> O <sub>2</sub> S |  | SA                  | 99%    |

<sup>a</sup>AK = AK Scientific, SA = Sigma-Aldrich, FS = Fisher Scientific, AO = Acros Organics

findings.<sup>17,23</sup> The experimental data found that  $\delta_D$ , which arises from atomic-induced dipole interactions rather than as a function of molecular structure (like  $\delta_p$  or  $\delta_H$ ), required a coefficient of 4 in the  $R_{i,j}$  equation to create a spherical shape to the interaction plot. Furthermore,  $R_{i,j}$  explicitly compares individual HSP values rather than the overall solubility vectors of the two components. With  $\Delta\delta_T$ , it is possible for a solvent–solute pairing to have drastically different values of multiple HSP components while maintaining similar values of  $\delta_T$ . For both methods, since the HSP values of a mixture are weighted by volume fractions of the individual components, mixing two individual solvents in different proportions can minimize  $R_{i,j}$  and  $\Delta\delta_T$  in order to maximize solubility.

## EXPERIMENTAL METHODS

**Solubility Determination.** FDCA solubility was determined for pure components (Table 1) as well as binary and ternary solvent blends using H<sub>2</sub>O, ACN, GVL, GBL, EtOH, MeOH, THF, DMSO, and SULF. The sample solution was prepared in a 3.0–10.0 g sample in a conical vial with weight determined using an analytical balance. FDCA was then added incrementally to the vial at room temperature (293 K, accuracy  $\pm 0.3$  K) while the solution was stirred at 800 rpm until FDCA was left visibly undissolved in the vial. Temperature was assessed using a K-type thermocouple and Omega Engineering OM-EL-USB-TC-LCD thermocouple data logger. If FDCA was still present in the vial after a minimum of 1 h of stirring, saturation was assumed to be reached<sup>6</sup> and the solution was allowed to settle for a minimum of 20 min, or until visibly

clear, before sampling. In the case of any uncertainty with solution conditions, additional stirring or settling time was allowed for up to 24 h. Procedures for the assessment of experimental conditions such as temperature ( $T$ ) and pressure ( $P$ ) are available in the Supporting Information.

For sampling, a 1.0 mL sample of the FDCA-saturated solvent was diluted with 18.2Ω H<sub>2</sub>O to prevent FDCA recrystallization in the high-performance liquid chromatography (HPLC) system. The amount of water added was determined by diluting the FDCA sample concentration to below the FDCA saturation point in pure water (a molarity of 0.0075). The diluted sample was filtered using a 0.2 μm membrane and then analyzed using an Agilent 1100 HPLC with DAD and RID detectors running trifluoroacetic acid buffer at a pH of 2 and flow rate of 0.6 mL/min on an Aminex HPX-87H (300 mm × 7.8 mm) column. Using the HPLC peak areas ( $A$ ), the mass fraction of FDCA ( $w_{\text{FDCA}}$ ) could be calculated as follows:

$$w_{\text{FDCA}} = \frac{0.001 \times k \times A \times D \times V \times M_{\text{W}}}{m_{\text{s}}} \quad (6)$$

where  $k$  is the HPLC standard calibration value,  $D$  is the dilution ratio,  $V$  is the total sample volume,  $M_{\text{W}}$  is the molecular weight of FDCA, and  $m_{\text{s}}$  is the total sample mass. Assessment of uncertainty on solubility values is reported in the Supporting Information.

**HSP Calculations.** The mixture HSP values for solvents were calculated using eqs 2–4 with pure component values

**Table 2. HSP Parameter Data (MPa<sup>1/2</sup>) for Pure Compounds at  $T = 293$  K as Determined Using the HSPiP Software where  $\Delta$  Calculates the Difference between the Pure Component and FDCA**

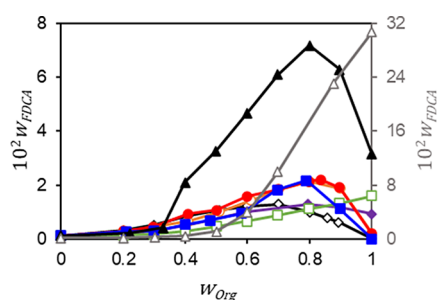
| chemical         | $\delta_D$ | $\delta_P$ | $\delta_H$ | $\delta_T$ | $\Delta\delta_D$ | $\Delta\delta_P$ | $\Delta\delta_H$ | $\Delta\delta_T$ | $R_{i,j}$ |
|------------------|------------|------------|------------|------------|------------------|------------------|------------------|------------------|-----------|
| FDCA             | 19.4       | 10.3       | 12.9       | 25.5       |                  |                  |                  |                  |           |
| DMSO             | 18.4       | 14.6       | 8.1        | 24.8       | 1                | 4.3              | 4.8              | 0.6              | 6.8       |
| GVL              | 16.8       | 11.4       | 6.7        | 21.4       | 2.6              | 1.1              | 6.2              | 4.1              | 8.2       |
| GBL              | 17.5       | 15.5       | 7.8        | 24.6       | 1.9              | 5.2              | 5.1              | 0.8              | 8.2       |
| SULF             | 18.1       | 16.8       | 8.4        | 26.1       | 1.3              | 6.5              | 4.5              | 0.6              | 8.3       |
| EtOH             | 15.8       | 8.8        | 19.4       | 26.5       | 3.6              | 1.5              | 6.5              | 1.1              | 9.8       |
| THF              | 16.7       | 4.9        | 5.8        | 18.3       | 2.7              | 5.4              | 7.1              | 7.1              | 10.4      |
| ACN              | 15.6       | 16.6       | 8.3        | 24.2       | 3.8              | 6.3              | 4.6              | 1.2              | 10.9      |
| MeOH             | 14.7       | 12.3       | 22.3       | 29.4       | 4.7              | 2                | 9.4              | 3.9              | 13.4      |
| H <sub>2</sub> O | 15.6       | 16         | 42         | 47.6       | 3.8              | 5.7              | 29.1             | 22.1             | 30.6      |

retrieved from the HSPiP software package (Table 2) at the same temperature as experiments were conducted, 293 K.<sup>24</sup>

**MATLAB Modeling Methods.** To determine ideal solvent blends based on minimizing  $R_{i,j}$ , a MATLAB program was created using version R2023a. The relevant solvent names and HSP parameters for the system under study were input into the code as a matrix. Once these variables were defined, the minimum  $R_{i,j}$  (eq 5) was found between FDCA and the stated solvent blend. The optimal mixture was identified using the “fmincon” function, which employs advanced nonlinear optimization methods to calculate the volume proportions of each solvent in the ideal blend. This function seeks to minimize the  $R_{i,j}$  value while being constrained by lower and upper bounds ranging from 0.0 to 1.0 for each solvent and a sum of the individual volume fractions totaling 1.0. The code outputs the names and volume fractions of each solvent that were then manually converted to a mass basis using densities. A full version of the code is available in the Supporting Information.

## RESULTS AND DISCUSSION

**Binary Aqueous/Organic Solvent Systems.** The eight organic solvents were studied in binary aqueous mixtures ranging from 20 to 90 wt % organic (Figure 1), and the maximum FDCA solubility for most solvents was approximately 2 wt % with the exception of THF (Figure 1; solid, black triangles) and DMSO (Figure 1; gray, unfilled triangles plotted on the secondary axis). THF solubilized a maximum of 7.2 wt % FDCA in a mixture of 20/80 w/w H<sub>2</sub>O/THF and



**Figure 1.** Plot of the mass fraction of FDCA solubilized ( $w_{\text{FDCA}}$ ) in varying binary mixtures of H<sub>2</sub>O and organic solvent (THF (triangle), SULF (square), MeOH (empty square), EtOH (diamond), ACN ( $\diamond$ ), GVL (circle), or GBL (empty circle)) with the organic mass fraction ( $w_{\text{Org}}$ ) on the horizontal axis. Solubility data for DMSO are shown on the secondary axis ( $\Delta$ ). Lines are provided to guide the eye. Raw data are provided in the Supporting Information (Tables S1–S8).

pure DMSO solubilized 30.7 wt % FDCA. Both results are significantly more than have been previously reported at higher temperatures,<sup>4–6</sup> or observed for the other solvents in this study.

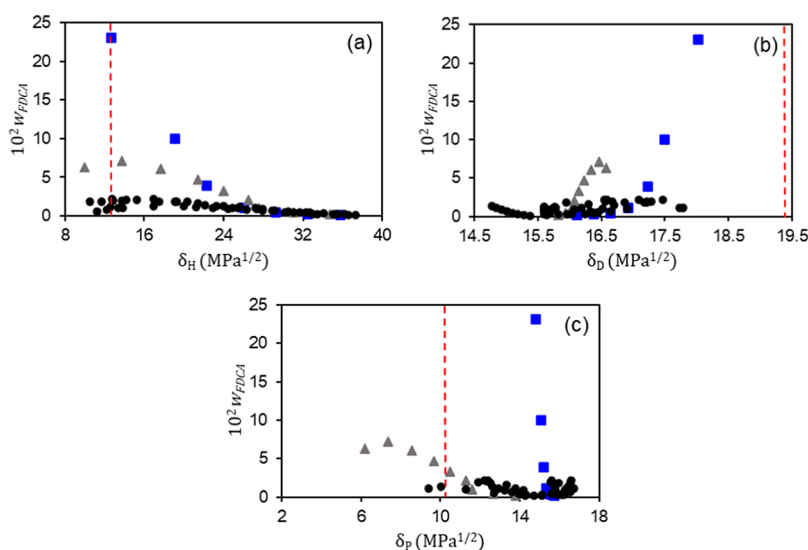
DMSO and MeOH had the highest FDCA solubility as pure solvents, which may be explained by their molecular structures. MeOH is a small molecule that readily forms hydrogen bonds with water, forming a framework of hydrogen bonds and thus increasing the overall volume of the solution.<sup>25</sup> This nonideal behavior is paired with positive heat of solution or an increase in overall system enthalpy. This increase moves the system further from a state of ideal mixing as previously defined in the theory section, meaning that as water is added the overall system enthalpy increases, leading to reduced solubility. The same behavior, of MeOH exhibiting the highest solubility as a pure component, has previously been observed by Ban et al. and was similarly correlated to hydrogen bonding interactions (Figure S2a).<sup>8</sup>

DMSO has also been shown to form strong hydrogen bonding networks with water, particularly at DMSO mass fractions less than 68 wt %.<sup>26</sup> This may explain why FDCA solubility in H<sub>2</sub>O/DMSO mixtures starts to exponentially increase in the DMSO mass fraction range of 60–70 wt % (Figure 1) since the hydrogen bond network may begin to weaken. When considering hydrogen bonding, Figure 2a shows the FDCA solubilities of all aqueous/organic solvent systems plotted against  $\delta_H$  of the solvent. For a given solvent system, the maximum solubility occurs near the  $\delta_H$  of FDCA (12.9; indicated by the red dashed line). Considering the other HSP parameters,  $\delta_D$  (Figure 2b) also shows an increasing trend as the  $\delta_D$  of the solvent approaches the  $\delta_D$  of FDCA, but in the case of  $\delta_P$ , no overall trends are seen for the solvent systems (Figure 2c).

The observation that the maximum FDCA solubility aligns closely with its  $\delta_H$  and  $\delta_D$  values indicates that adopting a more comprehensive approach using the differences in parameters, like  $R_{i,j}$  or  $\Delta\delta_T$ , may yield better correlations. This approach is supported by findings in the binary aqueous mixture data, where the highest FDCA solubility often matched the lowest  $R_{i,j}$  values (Figure 3). For  $\Delta\delta_T$ , there were slight deviations in some instances, as shown in Figure 3b,c,g,h.

Building on the findings of Zhuang et al.,<sup>6</sup> which identified the difference in total HSP ( $\Delta\delta_T$ ) as a predictor for FDCA solubility in aqueous/organic mixtures—a finding corroborated by this work—it was found that in seven of the eight binary systems currently studied,  $R_{i,j}$  offers a better or equivalent prediction of maximum FDCA solubility compared to  $\Delta\delta_T$  (Figure 3). Further comparison of the data presented in





**Figure 2.** Mass fraction of FDCA solubilized ( $w_{\text{FDCA}}$ ) in aqueous/organic binary solvent systems plotted versus (a)  $\delta_{\text{H}}$  (b)  $\delta_{\text{D}}$ , and (c)  $\delta_{\text{P}}$ . Markers represent H<sub>2</sub>O/DMSO (square), H<sub>2</sub>O/THF (triangle), and all other components (circle) with the dashed lines (---) representing the respective HSP value of FDCA.

the study by Zhuang et al.<sup>6</sup> also indicates a better correlation with  $R_{i,j}$  in three out of four cases (Figure S1). The same observation can be made of the data presented by Ban et al.,<sup>8</sup> wherein H<sub>2</sub>O/MeOH and H<sub>2</sub>O/EtOH data are seen to correlate high solubility to low  $R_{i,j}$  more strongly than to low  $\Delta\delta_{\text{T}}$  (Figure S2).

Aggregating the data from Figure 3 into a single plot reveals the correlation between  $R_{i,j}$  and FDCA solubility, as shown in Figure 4 using three markers: blue squares for H<sub>2</sub>O/DMSO mixtures, gray triangles for H<sub>2</sub>O/THF mixtures, and black circles for all other H<sub>2</sub>O/organic mixtures. As the  $R_{i,j}$  decreased from approximately 27 MPa<sup>1/2</sup>, the FDCA solubility increased across all solvent systems. However, while FDCA solubility consistently increased with decreasing  $R_{i,j}$  from approximately 20–13 MPa<sup>1/2</sup> across all solvents, the rate of increase becomes markedly varied below  $R_{i,j}$  values of 12 MPa<sup>1/2</sup>. The high solubilization in DMSO and THF may be explained by a combination of intramolecular solvent properties and intermolecular interactions with FDCA and H<sub>2</sub>O. Both solvents are highly polar and aprotic. While this alone does not distinguish them relative to the other solvents studied, both are known to report strong dipole–dipole interactivity and to readily form strong hydrogen bonds with water and organic compounds.<sup>27,28</sup> DMSO has further been identified as having an unusually high dielectric constant, which allows for easy charge separation and excellent solvation capacity,<sup>29</sup> and excels at disrupting crystalline lattices.<sup>27</sup> These combined effects may lead to a unique ability to solubilize much more FDCA than the other solvents studied.

While the trend in  $R_{i,j}$  with binary solvents suggests a correlation, the highest FDCA solubility was not consistently observed at the lowest  $R_{i,j}$  for pure solvents. In pure solvents, the FDCA solubility varied significantly, ranging from 0.02 wt % in ACN to 30.7 wt % in DMSO at 293 K. Notably, all solvents except ACN had higher solubilities than water (0.12 wt %), as listed in Table 3. Sulfolane, being solid at 293 K, could not be evaluated as a pure solvent. When considering HSP predictions by  $\Delta\delta_{\text{T}}$  and  $R_{i,j}$ , the pure solvents would be ordered differently and there were several notable discrepancies against HSP solubility predictions (Table 3).

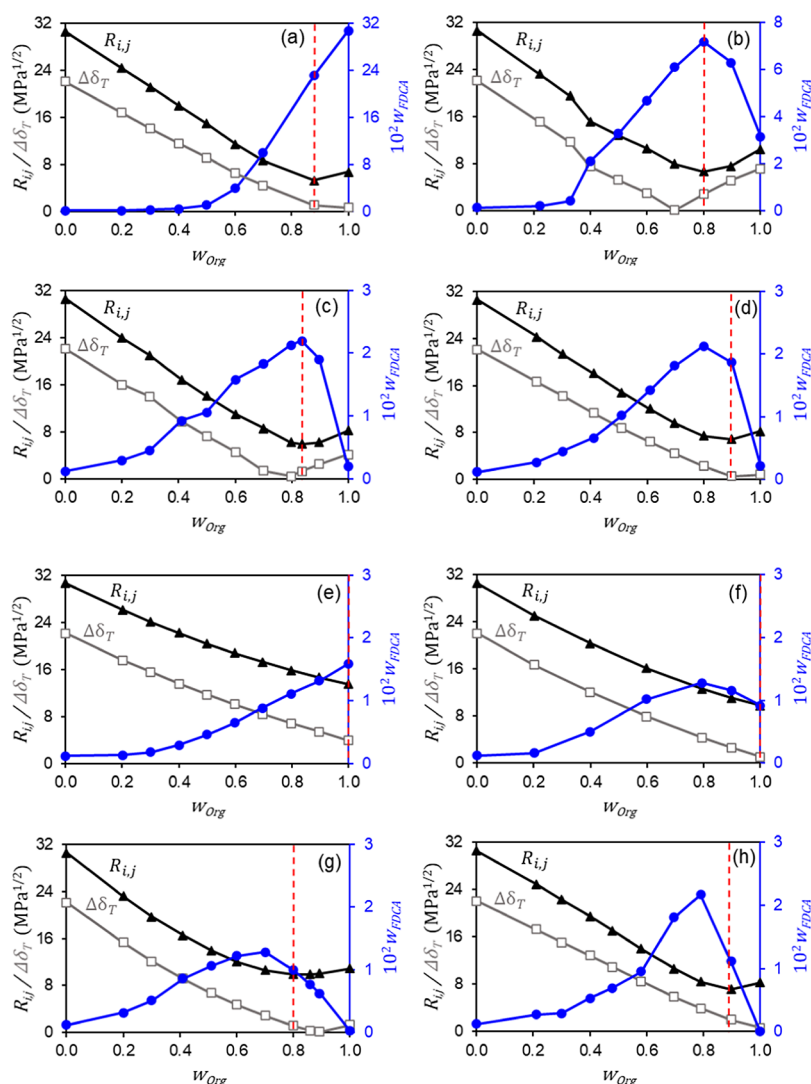
DMSO was predicted to have the highest FDCA solubility and, indeed, has the lowest  $\Delta\delta_{\text{T}}$  and  $R_{i,j}$ . However, GBL, GVL, MeOH, and ACN would be predicted to have higher solubilities based on their HSP values relative to the other solvents evaluated. In the case of MeOH and ACN, the previous literature mentions that molar volume can significantly impact solubility, stating that compounds with very small molar volumes may not conform to HSP predictions.<sup>21</sup> Specifically, small molecules like MeOH or ACN may exhibit solubility behaviors that diverge from those anticipated based on their HSP values. MeOH, at 0.380 nm in molecular diameter,<sup>30</sup> has been specifically cited as falling into this boundary effect category.<sup>21</sup>

Regardless of the FDCA solubility in pure components, in binary aqueous mixtures, a minimized  $R_{i,j}$  typically corresponds to the maximum or near-maximum FDCA solubility for a given aqueous/organic solvent system. Notably, H<sub>2</sub>O/DMSO and H<sub>2</sub>O/THF blends demonstrated particularly high FDCA solubilities, with low  $R_{i,j}$  values closely matching the points of highest FDCA solubility. While trends were observed between FDCA solubility and HSPs in binary mixtures, these trends did not extend to the prediction of FDCA solubility in pure solvents. This observation aligns with findings from nonaqueous binary mixture data as well (Figure S3, Table S12). The absence of a similar predictive trend in pure solvents and nonaqueous mixtures evaluated suggests that while HSPs can guide solubility optimization in aqueous binary mixtures, their applicability may be subject to greater variability in other solvent mixtures.

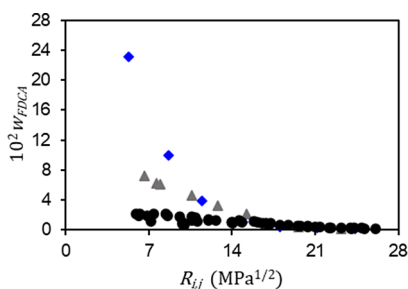
#### Ternary Aqueous/Organic/Organic Solvent Systems.

Due to the high FDCA solubility of DMSO and H<sub>2</sub>O/DMSO mixtures, ternary mixtures were evaluated that focused on H<sub>2</sub>O/DMSO combined with a second organic solvent of GVL, THF, or SULF. The use of DMSO in ternary mixtures can optimize the  $R_{i,j}$  of the solvent mixture due to the differences in HSPs, theoretically leading to higher solubility.

For the ternary H<sub>2</sub>O/DMSO/organic mixtures, FDCA solubilities ranged from less than 1 wt % at high  $R_{i,j}$  values to over 10 wt % for ternary mixtures that have an  $R_{i,j}$  less than 5, as seen in Figure 5. The ternary blends at 293 K exhibited



**Figure 3.**  $R_{i,j}$  (triangle),  $\Delta\delta_T$  (empty square), and the mass fraction of FDCA solubilized ( $w_{\text{FDCA}}$ ; circle, secondary axis) versus the mass fraction of organic ( $w_{\text{Org}}$ ) in binary mixtures of H<sub>2</sub>O and (a) DMSO, (b) THF, (c) GVL, (d) GBL, (e) MeOH, (f) EtOH, (g) ACN, or (h) SULF where the dashed line indicates the minima of  $R_{i,j}$  (dashed lines). Data collected at  $T = 293$  K and  $P = 0.1$  MPa.



**Figure 4.**  $R_{i,j}$  for H<sub>2</sub>O/DMSO (diamond), H<sub>2</sub>O/THF (triangle), all other H<sub>2</sub>O/organic (circle) mixtures plotted against mass fraction of FDCA solubilized ( $w_{\text{FDCA}}$ ).

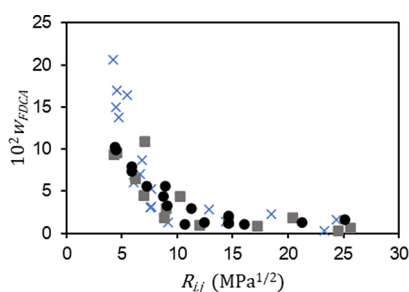
higher FDCA solubility compared to the binary blends studied by Zhuang et al. at higher temperatures (333 K).<sup>6</sup> For example, ternary blends containing 80 wt % total organic (DMSO and secondary organic) had FDCA solubilities exceeding 20 wt %. In the binary mixtures studied by Zhuang et al., those containing 80 wt % organic only reported a maximum of 7.9 wt % FDCA solubilized at 303 K (20/80 w/w H<sub>2</sub>O/THF) and 10.5 wt % at 333 K (20/80 w/w H<sub>2</sub>O/THF).<sup>6</sup> The other

**Table 3.** Amount of FDCA Solubilized in Each Pure Solvent Ranked from the Highest to Lowest FDCA Solubility at 293 K and the Ranking Predicted by  $\Delta\delta_T$  and  $R_{i,j}$  with 1 Being the Highest Expected Solubility and 8 Being the Lowest<sup>a</sup>

| chemical         | $10^2 w_{\text{FDCA}}$ | $\Delta\delta_T$ ranking | $R_{i,j}$ ranking |
|------------------|------------------------|--------------------------|-------------------|
| DMSO             | 30.7                   | 1                        | 1                 |
| THF              | 3.15                   | 7                        | 5                 |
| MeOH             | 1.59                   | 5                        | 7                 |
| EtOH             | 0.92                   | 3                        | 4                 |
| GBL              | 0.21                   | 2                        | 2                 |
| GVL              | 0.19                   | 6                        | 3                 |
| H <sub>2</sub> O | 0.12                   | 8                        | 8                 |
| ACN              | 0.02                   | 4                        | 6                 |

<sup>a</sup>Standard uncertainties were  $u(T) = 0.3$  K,  $u(P) = 0.1$  kPa and relative uncertainties were  $u_r(w_{\text{FDCA}}) = 0.061$  (for  $10^2 w_{\text{FDCA}} < 5$ ), 0.128 (for  $10^2 w_{\text{FDCA}} > 5$ ).

mixtures studied by Zhuang et al., H<sub>2</sub>O/DX, H<sub>2</sub>O/DME, and H<sub>2</sub>O/DGDE, had maximum solubilities of 5.1, 6.7, and 6.9 wt %, respectively, at 303 K. The FDCA solubilities reported in



**Figure 5.** Mass fraction of FDCA solubilized ( $w_{\text{FDCA}}$ ) in ternary mixtures of H<sub>2</sub>O/DMSO/organic, where the second organic was either GVL (circle), THF (×), or SULF (square), plotted against  $R_{i,j}$ .

this study are over a two-fold increase compared to these previously reported literature values.

As was the case with the binary solvent mixtures,  $R_{i,j}$  and FDCA solubility correlated (Figure 5) and indicated that minimizing  $R_{i,j}$  for a solvent system maximizes solubility. Across the three solvent systems, H<sub>2</sub>O/DMSO with GVL, THF, or SULF, the trend of maximum FDCA solubility at minimum  $R_{i,j}$  held true for the solvent blends studied (Table S13). There was a slight deviation in the case of H<sub>2</sub>O/DMSO/SULF at 20/40/40 w/w/w as the FDCA solubility was slightly higher than at the minimum  $R_{i,j}$  value, but still within the margin of error. The consistency of  $R_{i,j}$  being able to predict the maximum FDCA solubility for both binary and ternary aqueous mixtures could enable a more precise approach to solvent selection.

#### Solvent Selection Optimization Using MATLAB.

Building on the trends seen in the experimental data, a MATLAB model was developed that minimized  $R_{i,j}$  based on the volume fractions and HSPs of the solvents with FDCA as the solute. Initially, the code was used to find the minimum  $R_{i,j}$  for a mixture of H<sub>2</sub>O/DMSO/THF and determined mass fractions of 14/59/27 would maximize FDCA solubility. When the optimized ternary blend was evaluated experimentally, the FDCA solubility was found to be 20.7 wt %, which was the highest of any ternary blend studied (Figure 5). The two other ternary blends, H<sub>2</sub>O/DMSO/GVL and H<sub>2</sub>O/DMSO/SULF, as well as all binary systems studied, were inputted into the

code to find the minimum  $R_{i,j}$  blends and assess their solubility relative to experimentally found maxima (Table 4).

The MATLAB optimization code accurately predicted mixture compositions, often achieving results within 10 wt % of the composition determined experimentally and almost always within 15 wt %. There were two exceptions, which were H<sub>2</sub>O/EtOH and the ternary blend of H<sub>2</sub>O/DMSO/SULF. The challenge with the EtOH mixture may be due to its molar volume being near the boundary region for HSP predictions, as previously discussed, but the FDCA solubility was low as well, which has been previously reported as well.<sup>8</sup> For the ternary mixture involving SULF, the exclusion of SULF in the predicted mixture was due to its HSP values increasing  $R_{i,j}$ , which was an issue for the optimization code. From a research perspective, the optimization process narrows the range of experimental work needed, thereby allowing for more efficient experimentation. By limiting the experimental range to more targeted solvent blends, computational optimization can save time and resources in identifying optimal solvent mixtures to maximize FDCA solubility.

## CONCLUSIONS

This study marks a significant advancement in the understanding of FDCA solubility by systematically analyzing its behavior in pure, binary, and ternary solvent blends of H<sub>2</sub>O, ACN, DMSO, THF, SULF, GVL, GBL, MeOH, and EtOH at 293 K. The FDCA solubility was found to increase with decreasing values of both  $\Delta\delta_T$  and  $R_{i,j}$  within a set solvent system. Of these two HSP-based parameters, the correlation between FDCA solubility and  $R_{i,j}$  was stronger. Notably, mixtures containing DMSO were found to have the lowest  $R_{i,j}$  values and the highest FDCA solubility values (30.7 wt % maximum), followed by mixtures containing THF (7.2 wt % maximum). All other binary solvents investigated had less than 2.5 wt % of FDCA solubilized, but maximum solubility still correlated with the minimum  $R_{i,j}$ . The same trend was observed for ternary solvent blends, which saw solubilities exceeding 20 wt % at low values of  $R_{i,j}$ . In contrast, no correlation was found between using HSP parameters to predict the baseline solubility of pure solvent systems.

**Table 4.** Comparison of Experimental Maximum Solubility to MATLAB Predicted Maximum Solubility in Binary and Ternary Mixtures at  $T = 293$  K and  $P = 0.1$  MPa<sup>a</sup>

| chemical  | maximum solubility  |                       |                               |                       | difference between predicted <sup>b</sup> and experimental |                       |
|-----------|---------------------|-----------------------|-------------------------------|-----------------------|--|-----------------------|
|           | experimental        |                       | MATLAB Predicted <sup>b</sup> |                       |  |                       |
|           | $10^2(w_w/w_1/w_2)$ | $10^2w_{\text{FDCA}}$ | $10^2(w_w/w_1/w_2)$           | $10^2w_{\text{FDCA}}$ | $10^2w_1$  | $10^2w_{\text{FDCA}}$ |
| ACN       | 30/70/0             | 1.3                   | 17/83/0                       | ~1.0                  | -13  | -0.3                  |
| GBL       | 20/80/0             | 2.1                   | 12/88/0                       | ~1.9                  | -8   | -0.2                  |
| EtOH      | 21/79/0             | 1.4                   | 0/100/0                       | 0.9                   | -21  | -0.5                  |
| MeOH      | 0/100/0             | 1.6                   | 0/100/0                       | 1.6                   | 0  | 0                     |
| DMSO      | 0/100/0             | 30.7                  | 15/85/0                       | ~23.1                 | +15  | -7.6                  |
| GVL       | 16/84/0             | 2.2                   | 16/84/0                       | 2.2                   | 0  | 0                     |
| THF       | 20/80/0             | 7.2                   | 23/77/0                       | ~7.2                  | +3   | 0                     |
| SULF      | 21/79/0             | 2.2                   | 11/89/0                       | 1.1                   | -10  | -1.1                  |
| DMSO/GVL  | 20/60/20            | 10.3                  | 12/66/22                      |                       | -8/+6/+2   |                       |
| DMSO/THF  | 14/59/27            | 20.7                  | 14/59/27                      | 20.7                  | 0  | 0                     |
| DMSO/SULF | 20/40/40            | 10.9                  | 11/89/0                       | 1.1                   | -9/49/-40  | -9.8                  |

<sup>a</sup>Standard uncertainties were  $u(w_1, w_2, w_w) = 0.002$ ,  $u(T) = 0.3$  K,  $u(P) = 0.1$  kPa and relative uncertainties were  $u_r(w_{\text{FDCA}}) = 0.061$  (for  $10^2w_{\text{FDCA}} < 5$ ), 0.128 (for  $10^2w_{\text{FDCA}} > 5$ ). <sup>b</sup>The  $10^2w_{\text{FDCA}}$  "predicted" values represent the experimentally determined solubility at the predicted solvent composition.

The MATLAB code developed in this study effectively optimized solvent blends by minimizing  $R_{i,j}$ , predicting a narrow range of mass fractions that contained the maximum FDCA solubility for various solvent combinations. In the future, the code could readily be expanded to different solutes or solvents for additional applications. Identifying solvents that have increased solubility may allow for more efficient upgrading of chemicals such as FDCA and PEF, and the MATLAB code could be used to optimize a diverse range of solvent systems.

## ■ ASSOCIATED CONTENT

### SI Supporting Information

The Supporting Information is available free of charge at <https://pubs.acs.org/doi/10.1021/acsomega.4c03170>.

Error assessment; MATLAB code and code preparation; experimental data and HSP values for pure components and aqueous/organic mixtures; converted solubility data and figures comparing  $R_{i,j}$  and  $\Delta\delta_T$  for literature data (Zhuang et al.); converted solubility data and figures comparing  $R_{i,j}$  and  $\Delta\delta_T$  for literature data (Ban et al.); HSP values temperature-corrected to 303 K; data and figures assessing organic/organic binary mixtures; and experimental data and HSP values for ternary mixtures (PDF)

Error assessment and MATLAB code (PDF)

## ■ AUTHOR INFORMATION

### Corresponding Author

Stephanie G. Wettstein – Department of Chemical and Biological Engineering, Montana State University, Bozeman, Montana 59717, United States; [orcid.org/0000-0002-4437-3701](https://orcid.org/0000-0002-4437-3701); Email: [stephanie.wettstein@montana.edu](mailto:stephanie.wettstein@montana.edu)

### Authors

Jacob M. Molinaro – Department of Chemical and Biological Engineering, Montana State University, Bozeman, Montana 59717, United States  
Matthew R. Carroll – Department of Chemical and Biological Engineering, Montana State University, Bozeman, Montana 59717, United States  
Annabelle S. Young – Department of Chemical and Biological Engineering, Montana State University, Bozeman, Montana 59717, United States

Complete contact information is available at:

<https://pubs.acs.org/10.1021/acsomega.4c03170>

### Author Contributions

J.M.M.: Methodology, Data curation, Writing—Original manuscript preparation. A.S.Y.: Data curation. M.R.C.: Data curation and Methodology. S.G.W.: Conceptualization, Supervision, Funding acquisition, Methodology, Writing—Original manuscript preparation. All authors have given approval to the final version of the manuscript.

### Funding

National Science Foundation CBET, Grant No. 2230355.

### Notes

The authors declare no competing financial interest.

## ■ ACKNOWLEDGMENTS

The authors are grateful for the support of the National Science Foundation CBET, Grant No. 2230355. Any opinions,

findings, conclusions, or recommendations expressed in this material are those of the author(s) and do not necessarily reflect the views of the National Science Foundation. During the preparation of this work, the authors used ChatGPT in order to improve the readability and concision of the document. After using this tool/service, the authors reviewed and edited the content as needed and took full responsibility for the content of the publication. Additionally, the authors thank Nathaniel Cayen for his preliminary work gathering solubility data.

## ■ REFERENCES

- (1) Tamoor, M.; Samak, N. A.; Yang, M. H.; Xing, J. M. The Cradle-to-Cradle Life Cycle Assessment of Polyethylene terephthalate: Environmental Perspective. *Molecules* **2022**, *27*, No. 1599, DOI: 10.3390/molecules27051599.
- (2) Tiso, T.; Narancic, T.; Wei, R.; Pollet, E.; Beagan, N.; Schröder, K.; Honak, A.; Jiang, M. Y.; Kenny, S. T.; Wiercx, N.; Perrin, R.; Avérous, L.; Zimmermann, W.; O'Connor, K.; Blank, L. M. Towards bio-upcycling of polyethylene terephthalate. *Metab Eng.* **2021**, *66*, 167–178.
- (3) Rosenboom, J. G.; Hohl, D. K.; Fleckenstein, P.; Storti, G.; Morbidelli, M. Bottle-grade polyethylene furanoate from ring-opening polymerisation of cyclic oligomers. *Nat. Commun.* **2018**, *9*, 2701 DOI: 10.1038/s41467-018-05147-y.
- (4) Motagamwala, A. H.; Won, W. Y.; Sener, C.; Alonso, D. M.; Maravelias, C. T.; Dumesic, J. A. Toward biomass-derived renewable plastics: Production of 2,5-furandicarboxylic acid from fructose. *Sci. Adv.* **2018**, *4*, No. eaap9722, DOI: 10.1126/sciadv.aap9722.
- (5) Zhang, Y. Z.; Guo, X.; Tang, P.; Xu, J. Solubility of 2,5-Furandicarboxylic Acid in Eight Pure Solvents and Two Binary Solvent Systems at 313.15–363.15 K. *J. Chem. Eng. Data* **2018**, *63*, 1316–1324.
- (6) Zhuang, N. H.; Wang, J. C.; Ma, S.; Liu, Q.; Jia, W. L.; Yu, X.; Li, Z.; Yang, S. L.; Sun, Y.; Tang, X.; Zeng, X. H.; Lin, L. Determination of Solubility and Thermodynamic Analysis of Solubility Behavior of 2,5-Furandicarboxylic Acid in Water and Ether Binary Solvent System. *J. Chem. Eng. Data* **2023**, *68*, 726 DOI: 10.1021/acs.jced.2c00730.
- (7) Rose, H. B.; Greinert, T.; Held, C.; Sadowski, G.; Bommarius, A. S. Mutual Influence of Furfural and Furancarboxylic Acids on Their Solubility in Aqueous Solutions: Experiments and Perturbed-Chain Statistical Associating Fluid Theory (PC-SAFT) Predictions. *J. Chem. Eng. Data* **2018**, *63*, 1460–1470.
- (8) Ban, H. P. T.; Cheng, Y.; Wang, L.; Li, X. Solubilities of 2,5-Furandicarboxylic Acid in Binary Acetic Acid + Water, Methanol + Water, and Ethanol + Water Solvent Mixtures. *J. Chem. Eng. Data* **2018**, *63*, 1987–1993.
- (9) Megias-Sayago, C.; Lolli, A.; Ivanova, S.; Albonetti, S.; Cavani, F.; Odriozola, J. A. Au/AlO - Efficient catalyst for 5-hydroxymethylfurfural oxidation to 2,5-furandicarboxylic acid. *Catal. Today* **2019**, *333*, 169–175.
- (10) Sanabria, L.; Lederhos, C.; Quiroga, M.; Cubillos, J.; Rojas, H.; Martínez, J. J. Pt and Pd on activated carbon for oxidation of 5-hydroxymethylfurfural to 2,5-furandicarboxylic acid. *Ing. Compet.* **2017**, *19*, 37–43.
- (11) Hansen, C. M. *The Three Dimensional Solubility Parameter and Solvent Diffusion Coefficient: Their Importance In Surface Coating Formulation*; Technical University of Denmark, 1967.
- (12) Sánchez-Camargo, A. D.; Bueno, M.; Parada-Alfonso, F.; Cifuentes, A.; Ibáñez, E. Hansen solubility parameters for selection of green extraction solvents. *Trac-Trend Anal Chem.* **2019**, *118*, 227–237.
- (13) Lang, J. Y.; Wang, N.; Wang, X. H.; Wang, Y. L.; Chen, G. R.; Zhang, H. Applications of the Hansen Solubility Parameter for Cellulose. *Bioresources* **2021**, *16*, 7111–7120.
- (14) Ma, Q. Z.; Yu, C. Q.; Zhou, Y. R.; Hu, D. G.; Chen, J. B.; Zhang, X. J. A review on the calculation and application of lignin



Hansen solubility parameters. *Int. J. Biol. Macromol.* **2024**, *256*, No. 128506, DOI: 10.1016/j.ijbiomac.2023.128506.

(15) Job, A. L. S. S. M.; Umhey, C. E.; Hoo, K. A.; Wettstein, S. G. Using Artificial Neural Networks to Estimate Xylose Conversion and Furfural Yield for Autocatalytic Dehydration Reactions. *ACS Sustainable Chem. Eng.* **2022**, *10*, 177–181.

(16) Prasad, S. K. A. J.; Narishetty, V.; Kumar, V.; Dutta, S.; Ahmad, E. Recent advances in the production of 2,5-furandicarboxylic acid from biorenewable resources. *Mater. Sci. Energy Technol.* **2023**, *6*, 501–521.

(17) Yamamoto, H. A. S.; Hansen, C. M., In *Hansen Solubility Parameters 50th Anniversary Conference*; York, UK, 2017.

(18) Behboudi, E.; Soleymani, J.; Martinez, F.; Jouyban, A. Solubility of amlodipine besylate in acetonitrile plus water binary mixtures at various temperatures: Determination, modelling, and thermodynamics. *Phys. Chem. Liq.* **2022**, *60*, 892–909.

(19) Peña-Fernández, M. A.; Spanò, G.; Torres-Pabón, N. S.; Martínez, F. Solubility data and solubility parameters of barnidipine in different pure solvents. *Ars Pharm.* **2023**, *64*, 329–341.

(20) Sha, J.; Cao, Z. D.; Hu, X. R.; Huang, Z. B.; Chang, Y. G.; Wan, Y. M.; Sun, R. R.; Jiang, G. L.; He, H. X.; Li, Y.; Li, T.; Ren, B. Z. Solid-liquid equilibrium solubility measurement, model evaluation and Hansen solubility parameter of thiamethoxam in three binary solvents. *J. Chem. Thermodyn* **2021**, *158*, No. 106364, DOI: 10.1016/j.jct.2020.106364.

(21) Hansen, C. M. *Hansen Solubility Parameters: A User's Handbook*. 2nd ed.; CRC Press: Boca Raton, FL, 2007; p 519.

(22) Cheremisinoff, N. P. *Industrial Solvents Handbook*. 2nd ed.; CRC Press: Boca Raton, FL, 2003; p 344.

(23) Mathieu, D. Pencil and Paper Estimation of Hansen Solubility Parameters. *ACS Omega* **2018**, *3*, 17049–17056.

(24) Abbott, S. Y. H.; Hansen, C. M., In HSPiP, Ed.; [hansen-solubility.com/HSPiP](https://hansen-solubility.com/HSPiP): 2020.

(25) Concentrates: Methanol and water don't mix. *Chem. Eng. News* 29 April 2002, **2002**; p 24.

(26) Chand, A.; Chowdhuri, S. Effects of dimethyl sulfoxide on the hydrogen bonding structure and dynamics of aqueous N-methylacetamide solution. *J. Chem. Sci.* **2016**, *128*, 991–1001.

(27) Brayton, C. F. Dimethyl Sulfoxide (DMSO): A Review. *Cornell Veterinarian* **1986**, *76*, 61–90.

(28) Góralski, P. Interaction Site Enthalpies of the Phenol-Tetrahydrofuran Hydrogen-bond Complex in Various Solvents. *J. Chem. Soc., Faraday Trans.* **1988**, *1* (84), 4311–4316.

(29) MacGregor, W. S. *Ann. N.Y. Acad. Sci.* 1967; pp 3–12 vol. 141,

(30) Ikeda, A.; Abe, C.; Matsuura, W.; Hasegawa, Y., Development of Methanol Permselective FAU-Type Zeolite Membranes and Their Permeation and Separation Performances. *Membranes-Basel* **2021**, *11*.